

Accepted Manuscript

Experimental study of flexural behaviour of RC beams strengthened by longitudinal and U-shaped basalt FRP sheet

Wensu Chen, Thong M. Pham, Henry Sichembe, Li Chen, Hong Hao



PII: S1359-8368(17)30651-0

DOI: [10.1016/j.compositesb.2017.09.053](https://doi.org/10.1016/j.compositesb.2017.09.053)

Reference: JCOMB 5300

To appear in: *Composites Part B*

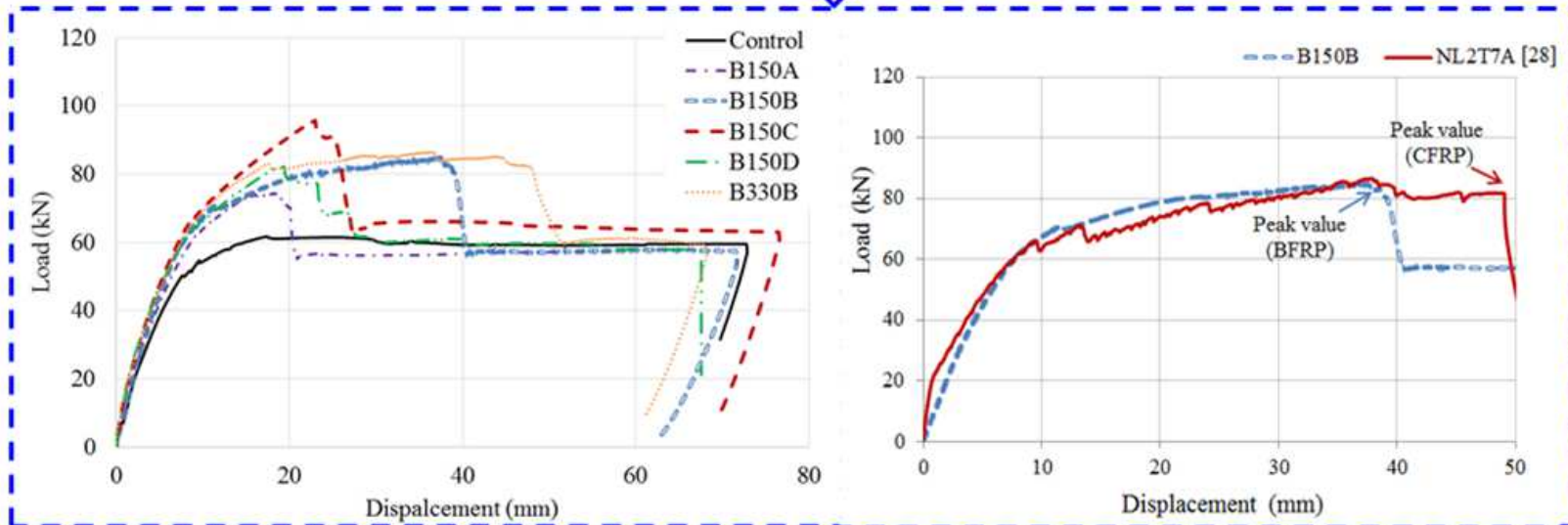
Received Date: 22 February 2017

Revised Date: 25 September 2017

Accepted Date: 25 September 2017

Please cite this article as: Chen W, Pham TM, Sichembe H, Chen L, Hao H, Experimental study of flexural behaviour of RC beams strengthened by longitudinal and U-shaped basalt FRP sheet, *Composites Part B* (2017), doi: 10.1016/j.compositesb.2017.09.053.

This is a PDF file of an unedited manuscript that has been accepted for publication. As a service to our customers we are providing this early version of the manuscript. The manuscript will undergo copyediting, typesetting, and review of the resulting proof before it is published in its final form. Please note that during the production process errors may be discovered which could affect the content, and all legal disclaimers that apply to the journal pertain.



1 **Experimental Study of Flexural Behaviour of RC Beams**
2 **Strengthened by Longitudinal and U-shaped Basalt FRP**
3 **Sheet**

4 Wensu Chen¹, Thong M. Pham¹, Henry Sichembe¹, Li Chen² and Hong Hao^{1*}

5 ¹*Centre for Infrastructural Monitoring and Protection,*

6 *School of Civil and Mechanical Engineering, Curtin University, Australia*

7 ²*PLA University of Science and Technology, Nanjing, 210007, China*

8 * Corresponding author's email: hong.hao@curtin.edu.au

9 **Abstract**

10 Fiber Reinforced Polymer (FRP) composite products such as Carbon FRP (CFRP) or
11 Glass FRP (GFRP) have been intensively studied for strengthening reinforced
12 concrete (RC) and masonry structures. It has been reported that FRP strengthening is
13 effective to enhance the structural load-carrying capacity. Basalt FRP (BFRP) is a
14 promising material for the application to structure strengthening with its advantages of
15 low cost, corrosion resistant and sound mechanical property, but only limited studies
16 of using Basalt FRP to externally strengthen RC beam are available in the literature.
17 This study is to experimentally explore the effectiveness of application of Basalt FRP
18 to strengthen RC beam under three-point bending test. The damage modes and

19 structural response of unstrengthened and BFRP strengthened RC beams were
20 recorded and identified. The effects of various BFRP wrapping schemes, U-jacket
21 anchorage and epoxy adhesives on the flexural capacity of RC beams were analysed
22 and discussed. In addition, the formulae used to predict the flexural behaviour of RC
23 beam strengthened by other FRP composites (e.g. CFRP/GFRP) were evaluated for
24 their applicability to Basalt FRP strengthening.

25 **Keywords:** Basalt FRP (BFRP), U-jacket, flexural, strengthening

26 **1 Introduction**

27 The use of FRP composites for structural strengthening was initiated in the late 1980s.
28 FRP has some advantages over traditional steel plates, such as high strength to weight
29 ratio, resistance to corrosion, flexibility and overall versatility [1]. The most
30 commonly used FRP in the industry is made of mainly carbon fibre (CFRP), glass
31 fibre (GFRP), aramid fibre (AFRP) and basalt fibre (BFRP). Various fibre composites
32 have been used to repair or strengthen structural components. Huang, et al. [2]
33 investigated the flexural behaviour of RC beams externally strengthened by natural
34 flax FRP composite. Dong, et al. [3] studied the flexural and flexural-shear
35 strengthening capacities of RC beams externally strengthened with FRP sheets. It was
36 found that flexural-shear strengthening scheme was more effective than the flexural
37 one in improving the stiffness and ultimate strength of RC beam. Choi, et al. [4]
38 reported debonding behaviour and structural performance of RC beams strengthened

39 by hybrid FRP composites. Skuturna and Valivonis [5] investigated the FRP
40 strengthening effect and failure modes of RC beams using various anchorage systems.
41 Yu and Wu [6] reported the performance of cracked steel beams reinforced by normal
42 modulus CFRP with different patch systems. Nguyen, et al. [7] used textile-reinforced
43 concrete to strengthen structural components of existing structures. Basalt fibre is an
44 environmentally friendly material which is made from melted basalt rock under high
45 temperature of 1400 °C and the molten rock is then extruded through small nozzles to
46 produce the fine fibre [8]. Basalt fibre is usually manufactured in a single process
47 known as continuous spinning, which allows for the production of short fibres and
48 continuous fibres [8]. The fibres can be made in the forms of chopped fibres, rebars
49 and continuous fibre sheets etc. Basalt FRP (BFRP) is a relative newcomer to FRP
50 composites, as compared with carbon FRP (CFRP) and glass FRP (GFRP). Although
51 it has superior characteristics such as high strength to weight ratio, sound ductility and
52 durability, high thermal resistance, and good corrosion resistance, and is cost effective
53 [9], its performance in structural strengthening has been less studied.

54 Externally bonded FRP has been intensively used in the flexural strengthening of RC
55 beams [10-16]. The strengthening of RC structural components by using FRP
56 laminates on the tension side has exhibited substantial enhancement to confinement,
57 stiffness and overall load carrying capacity [17]. Attari, et al. [18] reported that the
58 use of twin-layer GFRP sheets was effective in beam strengthening, exhibiting
59 flexural capacity gains as high as 114%. Sen and Reddy [19] used natural jute fibre

60 textile reinforced (JFRP) composite system to strengthen RC beams in flexure and
61 compared the effectiveness with using CFRP and GFRP strengthening systems. It was
62 reported that the ultimate flexural strength of the RC beams reinforced by JFRP,
63 CFRP and GFRP could be improved by 62.5%, 150% and 125%, respectively, with
64 full wrapping technique and by 25%, 50% and 37.5%, respectively with strip
65 wrapping scheme. However, only limited study of using Basalt FRP as an alternative
66 material to strengthen beam is available in literature. Sim, et al. [9] externally bonded
67 BFRP strips to the tension side of RC beams to increase the flexural load carrying
68 capacity. Both yielding and ultimate strength of the beam specimen increased up to
69 27%, depending on the number of layers applied. Şerbescu, et al. [20] investigated the
70 use of BFRP U-jacket strips as external shear reinforcement for RC beams, showing
71 efficiently delaying debonding failure at the plate end and reducing the brittleness of
72 failure.

73 FRP debonding (i.e. detachment of FRP from the concrete substrate) at the end or
74 intermediate crack (IC) debonding was identified as the frequently observed failure
75 mode [21-23]. Different anchorage measures have been used to suppress various
76 debonding failure to enhance the utilization efficiency of FRP material. Chahrour and
77 Soudki [24] studied the flexural behavior of RC beams strengthened by CFRP with
78 end anchorages to prevent peeling. Fu, et al. [25] externally bonded vertical and 45°
79 inclined FRP U-jackets at the plate ends as anchorage solution to mitigate the concrete
80 cover separation and intermediate crack debonding failure, which enhanced the

81 load-carrying capacity and ductility of beam. Smith and Teng [26] reported using
82 vertical FRP U-jacket at the end of the FRP soffit plate could lead to enhancement in
83 the ultimate load but the enhancement is limited. Lee and Lopez [27] used vertical or
84 inclined FRP U-jacket to enhance the strength of bonded joints with the range of 14%
85 to 118%. Pham and Hao [28] reported that using FRP U-wraps maximize the
86 capability of longitudinal FRP strips. Pham and Hao [29] investigated the
87 effectiveness and behaviour of 45° inclined U-jackets to the enhanced ability to arrest
88 flexural and shear cracks. Some design guidelines including ACI 440.2 R-08 [30]
89 specify the installation of vertical FRP U-jackets at plate end anchorage to suppress
90 concrete cover separation. However, a thorough comparison between the efficiency of
91 vertical and inclined U-jackets has not been presented. In this study, the longitudinal
92 and transverse strains of FRP U-jackets are presented and discussed.

93 As above-mentioned, basalt fibre is an alternative material for structural strengthening.
94 However, the testing data of BFRP strengthened beam is limited [9, 20]. More testing
95 data on BFRP strengthening is desired to supplement the current understandings for
96 more reliable and convincing results. The efficacy of beam strengthening by using
97 CFRP and BFRP has not been compared yet. The study on the effects of different
98 wrapping schemes using U-jacket anchorages and epoxy adhesives on BFRP
99 strengthening performance is limited. In addition, the design guidelines provided in
100 ACI 440.2R-08 [30] are applicable for CFRP/GFRP/AFRP materials while its

101 applicability of using BFRP to strengthen RC structure has not been verified yet. The
102 verification of the predications on BFRP strengthening is thus desired.

103 In this study, the effectiveness of different FRP anchors and epoxy adhesives in
104 strengthening RC beams in flexural was experimentally investigated. The changes of
105 the failure modes and the enhancement of the load-carrying capacity of RC beams
106 strengthened with BFRP were discussed. In addition, the design guideline proposed
107 by ACI 440.2R-08 for predicting the flexural behaviour of RC beams strengthened
108 with other FRP composites were evaluated against BFRP.

109 **2 Testing schemes**

110 **2.1 Specimen design**

111 In order to study the efficacy of BFRP strengthening beam under three-point bending,
112 six beams including one reference beam and five strengthened beams (namely B150A,
113 B150B, B150C, B150D and B330B) were prepared as detailed in Table 1. The
114 dimensions of the beams were 150 mm in width, 250 mm in height and 2200 mm in
115 length. All RC beams were reinforced with two deformed bars with 10-mm-diameter
116 at the tension side and two 12-mm-diameter bars at the compression side of the beam
117 in the longitudinal direction. All the six beams were designed to fail in flexural mode
118 with 10-mm-diameter steel stirrups at a spacing of 115 mm throughout the beam,
119 which indicated the shear resistance was much higher than the flexural resistance. The

120 details of the reinforcement are shown in Figure 1. The ready-mixed concrete with the
121 compressive strength of 40 MPa at 28 day age was used to cast the beams.

122 Based on the study conducted by Spadea, et al. [17], four wrapping schemes were
123 employed as shown in Figure 2. Each wrapping scheme comprised of either BFRP
124 soffit strips, U-jackets or a combination of them. In order to assess the significance of
125 epoxy adhesive, two different epoxies were also adopted to compare. Each specimen
126 was subjected to three point bending test until failure.

127 **2.2 Material properties**

128 The unidirectional BFRP sheet with the width of 100 mm and the density of 300 g/m²
129 was selected as external reinforcement. The nominal thickness of the BFRP sheet was
130 0.12 mm. The BFRP sheet had a tensile strength of 2100 MPa, tensile modulus of
131 77.9 GPa, and 2.1% tensile elongation [31]. To examine the strengthening efficacy by
132 using BFRP and CFRP, the experimental results from this study were compared with
133 RC beams strengthened with CFRP, reported in the study by Pham and Hao [28].
134 Accordingly, four layers of longitudinal BFRP strip were applied to ensure the equal
135 tensile force (i.e. width*thickness*tensile strength) provided by two layers of CFRP
136 strips with nominal thickness of 0.45 mm, as given in Table 2.

137 Premature debonding failure was a major issue of FRP reinforced concrete. The most
138 extensively used bonding agent for external FRP application was epoxy adhesive,
139 which consisted of two parts known as resin and hardener. To investigate the effect of

140 epoxy adhesives contributing to debonding of BFRP, two widely used epoxies i.e,
141 SikaDur 330 and West System 105-206 were adopted. As given in Table 3, the
142 elongation of the epoxy resin West System 105-206 was higher than that of SikaDur
143 330. Accordingly, FRP strengthened RC beams used West System 105-206 may
144 provide a higher load-carrying capacity than that of the beams used SikaDur 330.
145 However, it has been observed that debonding failure might initiate from the concrete
146 cover which was observed from the specimen B150D of this study so that the
147 adhesive does not necessarily govern the strength capacity of the beams. In addition,
148 the difference in the tensile modulus and elongation may also affect the effectiveness
149 of applying these adhesives. Therefore, the performance of using these adhesives was
150 unknown and investigated in this study.

151 **2.3 Specimen preparation**

152 Stress concentration can cause FRP premature rupture and lead to a low efficiency of
153 using FRP strengthening [32]. This phenomenon is highly dependent on the geometry
154 of the beam because stresses concentrate at sharp edges but well distribute along
155 gradual curves. Therefore, the edges of the beams were rounded at points which
156 would be in contact with the U-jackets using an angle grinder. The radius of the
157 rounded corners was about 25 mm. Careful surface preparation was carried out to
158 remove weak concrete before bonding FRP to the beams. A pneumatic needle gun
159 was used to carefully roughen the concrete surface. The accumulation of dust and
160 weak concrete resulting from grinding and needling processes was removed using a

161 pressurised air hose. The concrete surface was cleaned by acetone followed by
162 applying primer to the concrete surface before bonding with FRP. The wet layup
163 procedure was adopted for FRP bonding as shown in Figure 3. Prior to testing, all
164 beams as shown in Figure 4 were allowed a minimum of seven days for the epoxy
165 adhesive to cure.

166 **3 Testing setup and instrumentation**

167 The quasi-static testing setup included testing frame, A-frame supports, hydraulic jack,
168 LVDT, data acquisition system and other equipment as shown in Figure 5. A
169 three-point loading configuration using a roller and pin was used to provide simply
170 supported boundary condition. The effective span of the beams was 1.9 m. The beams
171 were loaded by using hydraulic jack with a loading rate at 0.6 mm/min. A number of
172 linear variable differential transformers (LVDT) and strain gauges were attached to
173 the beams at different locations to measure the deflection and strain values,
174 respectively. The load-displacement curves for each LVDT and the strain-time
175 histories for each strain gauge were recorded.

176 Debonding and rupture were two types of failure modes expected in these
177 strengthened beams. If debonding occurs it indicates that the high tensile strength of
178 FRP has been under-utilised. In order to monitor the longitudinal strains of BFRP, a
179 number of strain gauges were attached to the strengthened beams at the marked
180 locations i.e. the soffit of the beams (SGC “Strain Gauge Centre”; SGE1 “Strain

181 Gauge Eastern 1”) and the U-jackets SGU3L (“Strain Gauge U-jacket Longitudinal”)
182 as shown in Figure 6. The distribution of FRP strain along the beam soffit and the
183 FRP strain at failure, i.e. the strain corresponding to the FRP rupture or debonding can
184 be obtained.

185 **4 Test results and analysis**

186 The effects of bonding FRP strips to the beam soffit, adding U-jacket, vertical or
187 inclined U-jacket, U-jacket anchorage coverage and epoxy adhesive on the
188 strengthening performance are discussed and analysed through testing six specimens.
189 Table 4 summarises the key performance of each specimen. Failure modes including
190 cracking, FRP debonding and FRP rupture are presented and the data including
191 load-displacement and strain-time histories were recorded. The load-displacement
192 curves of all beams are presented in Figure 7.

193 **4.1 Control specimen**

194 The control specimen without strengthening experienced a flexural failure with severe
195 vertical cracks. Flexural cracking was symmetrical and hardly any abnormalities were
196 observed, confirming the correctness of the test setup. The cracks first appeared at
197 mid-span and extended towards the supports. They were all visually classified as
198 flexural cracks with no shear cracks appearing at any point during the test. All flexural
199 cracks were propagated vertically from the soffit of the beam as shown in Figure 8.

200 The control specimen achieved an ultimate applied load of 61.65 kN and a maximum
201 deflection of 16.70 mm at the ultimate load.

202 **4.2 Efficiency of the longitudinal strip**

203 The specimen B150A strengthened with BFRP strips at the soffit exhibited a similar
204 flexural cracking pattern to the control specimen as shown in Figure 9 (a). An ultimate
205 applied load of 74.37 kN was achieved with a corresponding mid-span deflection of
206 18.5 mm. B150A yielded a strength gain of 20.63% over the control specimen. After
207 the applied load peaked, B150A experienced intermediate debonding at the load of 71
208 kN and subsequently, complete debonding on the left side of the beam as shown in
209 Figure 9 (b). The debonding was caused by the failure of the concrete cover layer as
210 shown in Figure 9 (c and d). The strain gauges on the soffit strip of B150A recorded a
211 maximum strain of 0.96%, which was equal to 45.7% of the rupture strain from the
212 BFRP coupon tests. As shown in Figure 10, the maximum FRP strain at the mid-span
213 of 0.96% was recorded before debonding initiated and propagated from the mid-span.
214 This FRP strain of 0.96% was thus considered as the debonding strain. This
215 debonding strain was much higher than that of CFRP strengthened RC beams as
216 reported by Fu et al. (2016), where the debonding strain was recorded as 0.2%.

217 **4.3 Efficiency of U-jacket anchors**

218 To examine the efficiency of using U-jackets as anchorage, the specimen B150B was
219 prepared and tested. As shown in Figure 11, prior to failure, B150B experienced less

220 severe cracking and better concrete confinement than B150A. As shown in Figure 7,
221 an ultimate applied load of 84.9 kN with the corresponding deflection of 37.6 mm
222 were recorded, which represented a significant flexural strength gain of 37.7% over
223 the control specimen. Up to the ultimate load of B150A (i.e. 74.4 kN), B150B
224 exhibited a similar load-displacement curve, indicating a similar stiffness as Beam
225 B150A. Beyond this point, more deflection was achieved on B150B before failure,
226 indicating the U-jackets provided additional ductility. Beam B150B (with U-jackets)
227 had a strength increase of 14% over Beam B150A (without U-jackets). This increase
228 agreed well with experimental results from the studies by Ceroni and Pecce [33] and
229 Brena, et al. [34], where using CFRP U-wraps increased the strength capacity from 10%
230 to 57%. As shown in Figure 12, at an applied load of 84 kN, the strain gauge SGC
231 recorded a strain of over 1.8%, indicating that 85.7% of the BFRP's elongation strain
232 capacity was utilised. This data demonstrated BFRP yielded excellent elongation
233 strain efficiency. As shown in Figure 11, B150B experienced debonding of U-jackets
234 before the mid-span rupture of the soffit strip occurred at approximately 82.9 kN. This
235 failure mode demonstrated the effectiveness of the U-jackets in preventing the soffit
236 strip from debonding. The rupture of the longitudinal FRP strip instead of FRP
237 debonding was observed in the testing, indicating the BFRP material can be used
238 more efficiently.

239 **4.4 Efficiency of inclined U-jacket anchors**

240 Beam B150C was prepared to investigate the effectiveness of using 45° inclined
241 U-jackets. B150C was well confined with minimal cracking as shown in Figure 13.
242 The propagation of the flexural cracks in B150C was slow and not as widespread as
243 B150B. Prior to failure of the BFRP, minor flexural cracks appeared and were all less
244 than 1mm wide. B150C experienced compressive failure of concrete on the upward
245 face of the beam around the loading plate. As shown in Figure 7, B150C was
246 significantly less ductile than B150B as it experienced plastic deformation for a
247 smaller range of displacement before reaching the ultimate load. The stiffer behaviour
248 of B150C was visually apparent during the test, as it appeared to be minimally
249 deformed and very well confined throughout. Even after failure, B150C sustained a
250 higher constant load between 61kN and 63kN until the test stopped. The higher
251 residual strength of Beam B150C may be attributed to the inclined U-jackets which
252 were still well attached on the beam soffit and transferred tensile stresses to the beam
253 sides. Of all the tested beams, B150C recorded the highest ultimate load of 95.68 kN
254 with a corresponding deflection of 22.9 mm shown in Figure 7, which represented a
255 strength gain of 55.2% over the control beam and a 12.7% improvement with respect
256 to B150B reinforced with vertical U-jackets. This result was consistent with the
257 findings of Pham and Hao [29], who attributed the high strength associated with 45°
258 inclined U-jackets to their enhanced ability to arrest flexural and shear cracks. In
259 addition, placing the U-jackets at 45° meant that there was a slightly larger area of

260 BFRP bonded to the concrete and hence offered more resistance to the forces exerted
261 by the soffit strip.

262 In the course of testing B150C, cracking noises could only be heard after the applied
263 load exceeded 90 kN. When the applied load approached 95 kN, the cracking noises
264 intensified, indicating that failure was imminent. When the applied load peaked at
265 95.68 kN, a strain of 1.68% was recorded in the BFRP before mechanical destruction
266 of SGC occurred at 1.98% as shown in Figure 14. The strain of 1.98% and 1.68%
267 represented 94.3% and 80% of the rupture strain of the BFRP, respectively, which
268 indicated that BFRP material had an enhanced ability to exploit its high tensile
269 strength before debonding or rupture. After the applied load peaked and gradually
270 dropped to approximately 89 kN, the cracking noises intensified and a distinct tearing
271 noise was heard. The observation of the beam revealed that the BFRP soffit strip
272 ruptured completely at mid-span as shown in Figure 13 (c). Partial rupture of the soffit
273 strip at the location of SGE3 (between inclined U-jackets East 4 and 5) was observed
274 as shown in Figure 13 (d). It was worth mentioning that all the inclined U-jackets
275 were still well attached to the beam sides while vertical U-jackets debonded in Beam
276 B150B. The failure mode showed that utilizing U-jackets could effectively prevent
277 premature debonding and induce BFRP rupture mode, which was owing to the
278 effective anchorage of the BFRP soffit strip by the 45° inclined U-jackets, leading to
279 the more efficient exploitation of the tensile strength of BFRP.

280 4.5 Efficiency of U-jacket anchors at mid-span only

281 B150D with partial U-jackets anchorage coverage was prepared to investigate the
282 effect of U-jackets anchorage coverage on the strengthening performance. Aside from
283 the relatively late appearance of flexural cracks, B150D exhibited a symmetrical
284 cracking pattern. An ultimate load of 82.26 kN and deflection at ultimate load of 19.4
285 mm were recorded. B150D with partial anchorage exhibited a 33.4% flexural strength
286 gain over the control beam and a 3.1% flexural strength loss to B150B with full
287 U-jackets anchorage. This loss in flexural strength was considered to be minor,
288 indicating that the U-jackets located on the outer thirds of the beam contribute
289 minimally to the enhancement of flexural strength as compared to B150B. However,
290 owing to the widespread confinement and anchorage offered by the U-jackets applied
291 along the whole clear span of B150B, B150B was significantly more ductile than
292 B150D prior to failure as revealed in the load-displacement curves of Figure 7. In
293 addition, SGE2 out of the region of the U-jacket experienced higher strain than that of
294 SGE2 in Beams B150B and B150C. It showed that the U-jackets distributed at 1/3
295 span near the support help to control the strain and longitudinal stress near the support.
296 It is, therefore, concluded that using U-jackets for the whole beam span can
297 significant delay the debonding and increase the ductility, although it only marginally
298 increases the loading capacity of the beam strengthened with U-jackets only in the
299 mid-span region.

300 At an applied load of approximately 76 kN, B150D experienced debonding of the
301 soffit strip, followed by the complete debonding of U-jacket West UW2 and rupture
302 of U-jacket West UW1 as shown in Figure 15 (b/c). In order to classify the type of
303 debonding, BFRP samples were cut away from the soffit strip and U-jackets. As
304 shown in Figure 16 (a), the debonding of BFRP soffit strip occurred within the
305 concrete at the BFRP/concrete interface, indicating epoxy strength was higher than
306 the concrete tensile strength. Figure 16 (b) shows the U-jacket removed from the
307 beam. The U-jackets experienced the failure mode of severe concrete cover separation,
308 evidenced by the large pieces of concrete substrate attached on the removed U-jackets,
309 indicating the U-jackets can effectively transfer stress in the longitudinal BFRP strip
310 to the beam sides. The failure of the concrete cover separation was attributed to the
311 development of severe flexural cracks. A maximum soffit strain of 1.19% was
312 recorded by the strain gauge SGE3 as shown in Figure 17.

313 **4.6 Efficiency of different adhesives**

314 To study the effect of adhesives on the strengthening performance, Beam B330B with
315 the same wrapping scheme as B150B but using SikaDur 330 epoxy adhesive was
316 prepared. As shown in Figure 18, B330B exhibited severe cracking before failure and
317 no shear cracks were observed throughout the test. An ultimate load of 86.53 kN was
318 achieved with a corresponding mid-span deflection of 36.3 mm. These values were
319 close to the corresponding values of B150B. The flexural strength increase was 40.4%

320 and 1.9% over the control beam and Beam B150B, respectively. The strength gain
321 over B150B was found insignificant and can be treated as a variation in the
322 experimental tests. B330B and B150B had similar load-displacement curves until
323 failure occurred on B150B. The key difference between these two beams was the
324 higher ductility of B330B, which allowed deflecting approximately 25% more than
325 B150B before failure. However, it was expected that the beam B330B strengthened
326 with SikaDur 330 adhesive of higher tensile modulus should have yielded lower
327 ductility, but the tests results were opposite. The reason for this observation is not
328 exactly clear yet. Further study to confirm and explain the observed influences of
329 different epoxies are deemed necessary. Based on the testing observation in this study,
330 the increased ductility of B330B by using SikaDur 330 epoxy adhesive is a favourable
331 characteristic for FRP-concrete composites.

332 At the applied load of 85 kN, B330B experienced intermediate debonding at three
333 separate points along the soffit. Subsequently, UE5 began to debond and UE4
334 ruptured at the edge of the beam. This was followed by explosive debonding of the
335 soffit strip on the right side, resulting in the rupture of UE1, UE2 and UE3. As shown
336 in Figure 19, close examination of cut-outs from the debonded BFRP soffit strip and
337 U-jackets revealed a generally pure adhesive failure at the BFRP concrete interface,
338 leaving minimal damage to the concrete substrate.

339 B330B recorded a lower ultimate strain due to the lower tensile elongation capacity of
340 the SikaDur 330 epoxy resin. A maximum strain of only 1.4% and strain efficiency of

341 66.6% were recorded as shown in Figure 20. This fell short of 1.8% strain and 85.7%
342 strain efficiency of B150B. This was validated by the failure modes of B150B and
343 B330B. B150B failed by the BFRP rupture while B330B failed predominantly by
344 BFRP debonding. Due to the 4.5% tensile elongation capacity of the West System
345 105-206 epoxy applied to B150B being greater than the 2.1% tensile elongation
346 capacity of the BFRP, the BFRP soffit strip of B150B failed once 2.1 % strain was
347 exceeded. The relatively lower 0.9% tensile elongation capacity of the SikaDur 330
348 caused B330B BFRP debonding before the BFRP rupture. In general, the tested
349 beams failed by the FRP rupture or the debonding of the concrete cover layer,
350 indicating that the bonding strain of both adhesives were good.

351 **5 Discussions and comparisons**

352 **5.1 Failure modes and load-displacement curves**

353 All beams failed in the flexural mode. As demonstrated by the severe flexural
354 cracking, the control beam without strengthening failed in flexural tension. Beams
355 B150C and B150B failed in the form of BFRP strip rupture at mid-span soffit. This
356 was largely due to the sufficient anchorage supplied by the U-jackets which enabled
357 the beams to take advantage of the high tensile strength of BFRP. The rupture failure
358 of Beams B150B and B150C was demonstrated by high exploitation of the BFRP's
359 2.1% rupture strain and the sudden mechanical failure of the respective strain gauges.
360 Beams B150A, B150D and B330B failed in BFRP debonding of soffit strips. The

361 mechanism observed for all debonding was classified as failure of the concrete cover
362 layer. The debonding failure of Beams B150A, B150D and B330B was represented
363 by the low utilization of available rupture strain capacity of BFRP. Despite being
364 strengthened in the same wrapping scheme, Beams B330B and B150B experienced
365 different failure modes due to the lower elongation capacity and the higher tensile
366 modulus of SikaDur 330 epoxy adhesive as compared to those of West System
367 105-206.

368 The mid-span load-displacement curves of all tested beams were compared as shown
369 in Figure 7. Comparisons between the elastic deformation of the control beam and
370 that of the strengthened beams revealed that the contribution of the BFRP was
371 activated at approximately 40 kN (about 67% of the capacity of the reference beam).
372 Beyond the BFRP activation point, all strengthened beams were stiffer than the
373 control beam. A dramatic drop in strength was observed for all strengthened beams
374 immediately after the failure of BFRP. With respect to the ultimate load sustained by
375 the control beam, B150A, B150B, B150C, B150D and B330B exhibited flexural
376 strength gains of 20.6%, 37.7%, 55.2%, 33.4% and 40.4%, respectively. The
377 wrapping scheme C offered the greatest strength gain due to the enhanced ability of
378 inclined U-jackets to intercept severe shear and flexural cracks, which demonstrated
379 the effectiveness of BFRP U-jackets in anchoring the soffit strip and delaying
380 debonding. During the phase of plastic deformation, B150A, B150C and B150D
381 showed relatively low ductility. However, both B150B and B330B demonstrated

382 higher ductility than others and B330B exhibited the most ductile behavior among all
383 beams, which indicated epoxy adhesive had a more significant effect on ductility and
384 deformability than flexural strength.

385 **5.2 FRP strain**

386 The strain-time curves of the beams revealed strain values with respect to the BFRP's
387 ultimate strain of 2.1%. BFRP was not exempted from the inefficient exploitation of
388 FRP tensile strength that was commonly associated with the debonding failure linked
389 to CFRP, GFRP and AFRP. After close examination, all instances of debonding were
390 classified as failure of the concrete/BFRP interfacial and the epoxy adhesive. B150B
391 and B150C failed by the rupture of the longitudinal BFRP strips. It was reflected by
392 the high strains recorded by both beams, with B150B using a remarkable 95.7% of the
393 available rupture strain prior to the rupture at 2.1%. Despite their similar wrapping
394 schemes, B150B and B330B experienced different failure modes due to different
395 elongation strain capacity and tensile modulus of epoxy used in the two beams, as
396 discussed previously. SikaDur 330 failed before the BFRP could rupture. It should be
397 noted that the debonding strain can be up to 1.19% by using BFRP and U-jacket
398 anchorages, which was much higher than 0.4~0.6% by using CFRP as reported in the
399 study [28]. The advantage of using BFRP as an alternative strengthening material was
400 presented. It should be noted that the debonding stress corresponding to the debonding
401 strain can be used in section analyses. The corresponding stress was calculated based

402 on bond strength model, e.g., Teng et al.'s (2003) model [23] as adopted by ACI
403 440.2R-08 [30]. More details and discussion can be found in the previous study by Fu
404 [35].

405 To examine the contribution of the U-jackets, strain gauges were bonded to the
406 U-jackets in two directions as shown in Figure 10, Figure 12, Figure 14, Figure 17
407 and Figure 20. Vertical U-jackets debonding at failure was observed in Beams B150B
408 and B150D and vertical U-jackets ruptured in Beam B150D leading to the debonding
409 in the longitudinal strip as shown in Figure 15 (c). Interestingly, all the inclined
410 U-jackets of Beam B150C did not debond or rupture but the longitudinal FRP strip
411 ruptured, indicating the superior performance of inclined U-jackets. In Beam B150B,
412 the longitudinal and transverse strains of the debonded U-jacket (i.e. SGU5L and
413 SGU5T) were approximately 0.4% and 0.3%, respectively. Meanwhile, the maximum
414 longitudinal strain of the inclined U-jacket of Beam B150C was recorded as about 0.5%
415 at SGU5L. This higher value of the longitudinal strain of the inclined U-jacket
416 compared to the vertical U-jacket resulted in higher load-carrying capacity of Beam
417 B150C than that of Beam B150B. U-jackets have proven their ability to delay the
418 debonding of longitudinal strips. However, if the number of U-jacket anchors was not
419 enough to transfer stress in longitudinal strips to the beam side, they might fail in
420 shear in Beam B150 D as shown in Figure 15. The maximum transverse strain in
421 vertical U-jackets was recorded as high as 1.19% as shown in Figure 17. Therefore, it
422 again showed the advantage of using inclined U-jackets, where a portion of transverse

423 stress caused by the deformation of the longitudinal strip can be resisted by the
424 U-jacket in its longitudinal direction. In addition, ductility index, which is defined as
425 the mid-span deflection at failure divided by the mid-span deflection at the yielding of
426 steel tension bars, was used to quantify the ductility of beams [35]. As given in Table
427 4, the ductility index for the specimens B150A, B150B, B150C, B150D and B330B
428 were 2.16, 3.32, 2.43, 2.23 and 4.08, with the increase of 3.8%, 59.6%, 16.8%, 7.2%
429 and 96.2% over the control beam, respectively.

430 **5.3 Efficacy comparison with CFRP**

431 To compare the efficacy of using CFRP and BFRP, the beam design in this study was
432 approximately the same as that in the study by Pham and Hao [28]. The efficacy of
433 BFRP for the flexural strengthening of RC beam was therefore compared with CFRP
434 strengthened beams by Pham and Hao [28]. Four layers of longitudinal BFRP strips
435 were applied to ensure the equal tensile force (i.e. cross section*tensile strength)
436 provided by two layers of CFRP strips. The BFRP/CFRP-strengthened beams showed
437 the maximum loads 84.9 kN and 86.6 kN, respectively. These two strengthened
438 beams also showed similar stiffness until failure as shown in Figure 21. It is noted that
439 the energy absorption is defined as the area under the load-displacement curves of the
440 beams up to failure of the longitudinal strips (i.e. a significant drop in the curves)
441 since the contribution of FRP to the strengthened beam's capacity is of interest in this
442 study. The energy absorptions of BFRP and CFRP-strengthened beams at the ultimate

443 loads were 2.4 kNm and 3.2 kNm, respectively. However, BFRP has great potential as
 444 strengthening material compared to other materials (e.g. CFRP, GFRP, and AFRP)
 445 due to its cost-effectiveness.

446 **6 Verification against guideline**

447 The guideline ACI 440.2R-08 [30] is adopted for analytical verification to predict the
 448 ultimate moment capacity (M_u) of a beam with wrapping scheme A (i.e. B150A). To
 449 make comparisons between the analytical and experimental results, the ultimate
 450 applied load recorded in the tests is expressed as the ultimate bending moment, which
 451 is 33.48 kNm. Currently, ACI 440.2R-08 [30] is only applicable to CFRP, GFRP and
 452 AFRP materials and the wrapping scheme A. The predication on load carrying
 453 capacity of B150A using ACI 440.2R-08 is expressed as follows:

$$454 \quad M_u = 0.85f'_c b\beta c \left(c - \frac{\beta}{2}c \right) + A'_s E_s \varepsilon'_s (c - d_c) + A_s f_y (d - c) + \psi A_f E_f \varepsilon_{db} (h - c) \quad (1)$$

455 where ψ is the reduction factor on the contribution of FRP to beam strength, β
 456 is a coefficient defined in ACI318-08 [36], c is the depth of concrete compression
 457 block; A_f , A_s and A'_s represent the cross section area of FRP reinforcement,
 458 tension rebar and compression rebar, respectively; ε_s and ε'_s represent the strain in
 459 tension rebar and compression rebar; ε_{db} stands for debonding strain of FRP.

460 The ultimate moment capacity predicted by ACI 440.2R-08 [30] is 31.1 kNm, which
 461 underestimates the testing ultimate moment capacity (M_u) by 7%, with an error

462 margin less than 10%. Therefore, the beam using wrapping scheme A with BFRP
463 composites can yield reasonably sound prediction by using ACI 440.2R-08 [30]. ACI
464 440.2R-08 also gives the prediction of the FRP debonding strain (ϵ_{fd}) of B150A as
465 follows:

$$466 \quad \epsilon_{fd} = 0.41 \sqrt{\frac{f'_c}{nE_f t_f}} \leq 0.9\epsilon_{fu} \quad (2)$$

467 where f'_c is the compressive stress in concrete; n is the number of plies of FRP
468 reinforcement. E_f and t_f represent tensile modulus and nominal thickness of one
469 ply of FRP reinforcement. After calculation, the FRP debonding strain ϵ_{fd} is 1.32%.
470 In the tests, the FRP debonding strain of B150A was measured as 0.96 %, which is
471 lower than the value predicted by ACI 440.2R-08 [30].

472 7 Conclusions

473 This study presents the performance of RC beams strengthened with BFRP against
474 quasi-static loading. The experimental results show that external bonding of BFRP
475 sheets is an effective method of enhancing flexural strength of reinforced concrete
476 beams. Failure mode is highly dependent on the degree of anchorage offered by the
477 wrapping schemes and the mechanical properties of the epoxy adhesive. The findings
478 in this study are summarized as follows:

- 479 1. Using U-jackets as an anchor system can change the failure mode from FRP
480 debonding to FRP rupture. By using the same amount of materials, inclined U-jackets
481 (highly recommended) is much more efficient than vertical U-jackets.
- 482 2. Using U-jackets anchorage is able to provide significant anchorage and delaying
483 debonding by increasing the load-carrying capacity of B150A from 20% to 37.8% of
484 B150B with U-jackets anchorages.
- 485 3. Full coverage of U-jackets anchorage performs slightly better than partial
486 coverage of U-jackets anchorage by enhancing the load-carrying capacity of B150D
487 from 33.4% to 37.8% of B150B with full coverage of U-jackets anchorages.
- 488 4. Using inclined U-jackets is more effective than vertical U-jacket with the
489 load-carrying capacity increased from 37.7% of B150B to 55.2% of B150C anchored
490 with inclined U-jackets.
- 491 5. The Beam B330B with SikaDur 330 adhesive has slightly higher load-carrying
492 capacity but less ductility than the Beam B150B with West System 105-206 adhesive.
- 493 6. ACI 440.2R-08 predicts the ultimate moment capacity of B150A with error
494 margin of 7% and the formulae were therefore deemed applicable to BFRP
495 strengthened beam at the soffit.

496 In addition, as evidenced by the recorded high strain values, BFRP shows its ability to
497 make use of its high tensile strength more efficiently than carbon, glass and aramid
498 FRPs. Coupled with its low price, excellent heat resistance and lower environmental
499 impact, the use of BFRP for flexural strengthening of RC structures is justifiable and
500 ideal where the very high tensile strength of CFRP is not necessary. After the current

501 quasi-static study, the performance of RC beams strengthened with BFRP sheet
502 subjected to dynamic loading will be investigated to have a more comprehensive
503 understandings of the effectiveness of BFRP strengthening of concrete beams
504 subjected to both static and dynamic loads.

505 **Acknowledgements**

506 The authors would like to acknowledge Australian Research Council (Grant No.
507 LP150100259) for financial support to carry out this study. The authors also
508 acknowledge the technical support from Arne Bredin, Mick Ellis, Ashley Hughes,
509 Luke English, Rob Walker, and Craig Gwyther at Curtin University.

510 **References**

- 511 [1] M. Erki, U. Meier, Impact loading of concrete beams externally strengthened with
512 CFRP laminates, *J. Composite Constr.*, 3 (1999) 117-124.
- 513 [2] L. Huang, B. Yan, L. Yan, Q. Xu, H. Tan, B. Kasal, Reinforced concrete beams
514 strengthened with externally bonded natural flax FRP plates, *Composites Part B:
515 Engineering*, 91 (2016) 569-578.
- 516 [3] J. Dong, Q. Wang, Z. Guan, Structural behaviour of RC beams with external
517 flexural and flexural–shear strengthening by FRP sheets, *Composites Part B:
518 Engineering*, 44 (2013) 604-612.
- 519 [4] E. Choi, N. Utui, H.S. Kim, Experimental and analytical investigations on
520 debonding of hybrid FRPs for flexural strengthening of RC beams, *Composites Part
521 B: Engineering*, 45 (2013) 248-256.
- 522 [5] T. Skuturna, J. Valivonis, Experimental study on the effect of anchorage systems
523 on RC beams strengthened using FRP, *Composites Part B: Engineering*, 91 (2016)
524 283-290.

- 525 [6] Q.-Q. Yu, Y.-F. Wu, Fatigue Strengthening of Cracked Steel Beams with
526 Different Configurations and Materials, *J. Composite Constr.*, (2016) 04016093.
- 527 [7] T.H. Nguyen, X.H. Vu, A.S. Larbi, E. Ferrier, Experimental study of the effect of
528 simultaneous mechanical and high-temperature loadings on the behaviour of
529 textile-reinforced concrete (TRC), *Constr Build Mater*, 125 (2016) 253-270.
- 530 [8] V. Fiore, T. Scalici, G. Di Bella, A. Valenza, A review on basalt fibre and its
531 composites, *Composites Part B: Engineering*, 74 (2015) 74-94.
- 532 [9] J. Sim, C. Park, D.Y. Moon, Characteristics of basalt fiber as a strengthening
533 material for concrete structures, *Composites Part B: Engineering*, 36 (2005) 504-512.
- 534 [10] T.M. Pham, L.V. Doan, M.N.S. Hadi, Strengthening square reinforced concrete
535 columns by circularisation and FRP confinement, *Constr Build Mater*, 49 (2013)
536 490-499.
- 537 [11] J. Teng, J.-F. Chen, S.T. Smith, L. Lam, FRP: strengthened RC structures,
538 *Frontiers in Physics*, (2002).
- 539 [12] H. Rahimi, A. Hutchinson, Concrete beams strengthened with externally bonded
540 FRP plates, *J. Composite Constr.*, 5 (2001) 44-56.
- 541 [13] H. Saadatmanesh, M.R. Ehsani, RC beams strengthened with GFRP plates. I:
542 Experimental study, *J. Struct. Eng.*, 117 (1991) 3417-3433.
- 543 [14] S.T. Smith, J. Teng, FRP-strengthened RC beams. I: review of debonding
544 strength models, *Eng. Struct.*, 24 (2002) 385-395.
- 545 [15] T.M. Pham, H. Hao, Review of Concrete Structures Strengthened with FRP
546 Against Impact Loading, *Structures*, 7 (2016) 59-70.
- 547 [16] T.C. Triantafillou, N. Plevris, Strengthening of RC beams with epoxy-bonded
548 fibre-composite materials, *Mater. Struct.*, 25 (1992) 201-211.
- 549 [17] G. Spadea, F. Bencardino, F. Sorrenti, R.N. Swamy, Structural effectiveness of
550 FRP materials in strengthening RC beams, *Eng. Struct.*, 99 (2015) 631-641.
- 551 [18] N. Attari, S. Amziane, M. Chemrouk, Flexural strengthening of concrete beams
552 using CFRP, GFRP and hybrid FRP sheets, *Constr Build Mater*, 37 (2012) 746-757.

- 553 [19] T. Sen, J.H.N. Reddy, Strengthening of RC beams in flexure using natural jute
554 fibre textile reinforced composite system and its comparative study with CFRP and
555 GFRP strengthening systems, *International Journal of Sustainable Built Environment*,
556 2 (2013) 41-55.
- 557 [20] A. Şerbescu, P. Kypros, N. Țăranu, The Efficiency of Basalt Fibres in
558 Strengthening the Reinforced Concrete Beams, *The Bulletin of the Polytechnic
559 Institute of Jassy, Construction. Architecture Section*, 52 (2006) 47-58.
- 560 [21] J. Bonacci, M. Maalej, Behavioral trends of RC beams strengthened with
561 externally bonded FRP, *J. Composite Constr.*, 5 (2001) 102-113.
- 562 [22] Yao, Teng, Lam, Experimental study on intermediate crack debonding in
563 FRP-strengthened RC flexural members, *Adv. Struct. Eng.*, 8 (2005) 365-396.
- 564 [23] J. Teng, S.T. Smith, J. Yao, J. Chen, Intermediate crack-induced debonding in
565 RC beams and slabs, *Constr Build Mater*, 17 (2003) 447-462.
- 566 [24] A. Chahrour, K. Soudki, Flexural response of reinforced concrete beams
567 strengthened with end-anchored partially bonded carbon fiber-reinforced polymer
568 strips, *J. Composite Constr.*, 9 (2005) 170-177.
- 569 [25] B. Fu, J.G. Teng, J.F. Chen, G.M. Chen, Y.C. Guo, Concrete Cover Separation in
570 FRP-Plated RC Beams: Mitigation Using FRP U-Jackets, *J. Composite Constr.*,
571 (2016) 04016077.
- 572 [26] S.T. Smith, J.G. Teng, Shear-bending interaction in debonding failures of
573 FRP-plated RC beams, *Adv. Struct. Eng.*, 6 (2003) 183-199.
- 574 [27] J. Lee, M.M. Lopez, Characterization of FRP Uwrap Anchors for Externally
575 Bonded FRP-Reinforced Concrete Elements: An Experimental Study, *J. Composite
576 Constr.*, 20 (2016).
- 577 [28] T.M. Pham, H. Hao, Behavior of FRP Strengthened RC Beams under Static and
578 Impact Loads, *Int J Protective Struct*, (2016).
- 579 [29] T.M. Pham, H. Hao, Impact Behavior of FRP-Strengthened RC Beams without
580 Stirrups, *J. Composite Constr.*, 20 (2016).

- 581 [30] A.C. Institute, Guide for the Design and Construction of Externally Bonded FRP
582 Systems for Strengthening Concrete Structures, in: ACI 440.2 R-08, American
583 Concrete Institute, 2008.
- 584 [31] W. Chen, H. Hao, M. Jong, J. Cui, Y. Shi, L. Chen, T.M. Pham, Quasi-static and
585 dynamic tensile properties of basalt fibre reinforced polymer, Composites Part B:
586 Engineering, 125 (2017) 123-133.
- 587 [32] A. Mutalib, Damage assessment and prediction of FRP strengthened RC
588 structures subjected to blast and impact loads, in, University of Western Australia,
589 2011.
- 590 [33] F. Ceroni, M. Pecce, Evaluation of bond strength in concrete elements externally
591 reinforced with CFRP sheets and anchoring devices, J. Composite Constr., 14 (2010)
592 521-530.
- 593 [34] S.F. Brena, R.M. Bramblett, S.L. Wood, M.E. Kreger, Increasing flexural
594 capacity of reinforced concrete beams using carbon fiber-reinforced polymer
595 composites, ACI Struct J, 100 (2003) 36-46.
- 596 [35] B. Fu, Debonding failure in FRP-strengthened RC beams: prediction and
597 suppression, in, The Hong Kong Polytechnic University 2016.
- 598 [36] ACI_Committee, Building code requirements for structural concrete (ACI
599 318-08) and commentary, in, American Concrete Institute, 2008.

Table 1 Description of testing specimens

Specimen	Epoxy adhesive	Wrapping scheme	Wrapping scheme description
Control	N/A	N/A	N/A
B150A	West System 105-206	A	4 layer soffit strip
B150B	West System 105-206	B	4 layer soffit strip/ 2 layer vertical U-jackets throughout length
B150C	West System 105-206	C	4 layer soffit strip/2 layer 45° U-jackets throughout length
B150D	West System 105-206	D	4 layer soffit strip/ 2 layer vertical U-jackets central third of length
B330B	SikaDur 330	B	4 layer soffit strip/ 2 layer vertical U-jackets throughout length

Table 2 Mechanical properties of BFRP and CFRP materials

Parameter	300 g/m ² BFRP	340 g/m ² CFRP*
Width (mm)	100	75
Nominal thickness (mm)	0.12	0.45
Tensile strength (MPa)	1684	1500
Tensile force per layer	25200	50625
Failure strain %	2.1	1.65
FRP layers	4	2

*Data is adopted from the previous study [28].

Table 3 Mechanical properties of epoxy adhesives

Mechanical properties	SikaDur 330	West System 105-206
Required Curing (Days)	7 at 23°C	4 at 16°C
Tensile Strength (MPa)	30	50.3
Tensile Modulus (MPa)	4500	3171.6
Tensile Elongation (%)	0.9	4.5
Resin/ Hardener Mix Ratio	4:1 by Weight	5:1 by Volume

Table 4 Summary of testing data

Specimen	Control	B150A	B150B	B150C	B150D	B330B
Ultimate load (kN)	61.65	74.37	84.90	95.68	82.26	86.53
Load capacity increase (%)	-	20.6	37.7	55.2	33.4	40.4
Deflection at ultimate load (mm)	17.33	18.50	37.56	22.90	19.41	36.30
Deflection at the yielding of steel tension bars (mm)	8.04	8.54	11.30	9.41	8.70	8.90
Ductility index	2.08	2.16	3.32	2.43	2.23	4.08
Soffit debonding strain (%)	-	0.96	N/A	N/A	1.19	N/A
Max strain in soffit strip before failure (%)	-	0.96	1.80	1.68	1.19	1.40
Strain efficiency (%)	N/A	45.7	85.7	80.0	56.7	66.7

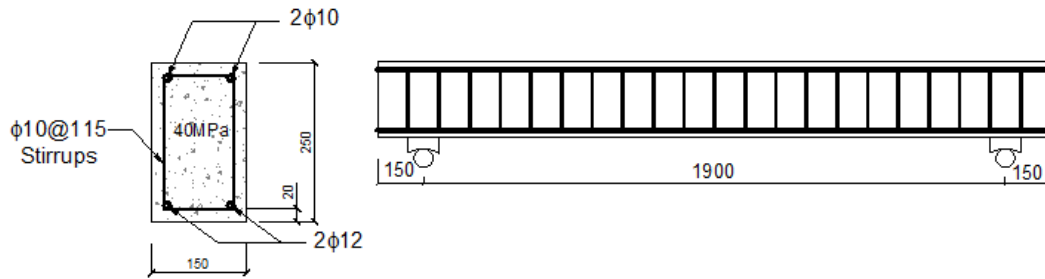


Figure 1 Dimension and configuration of RC beam

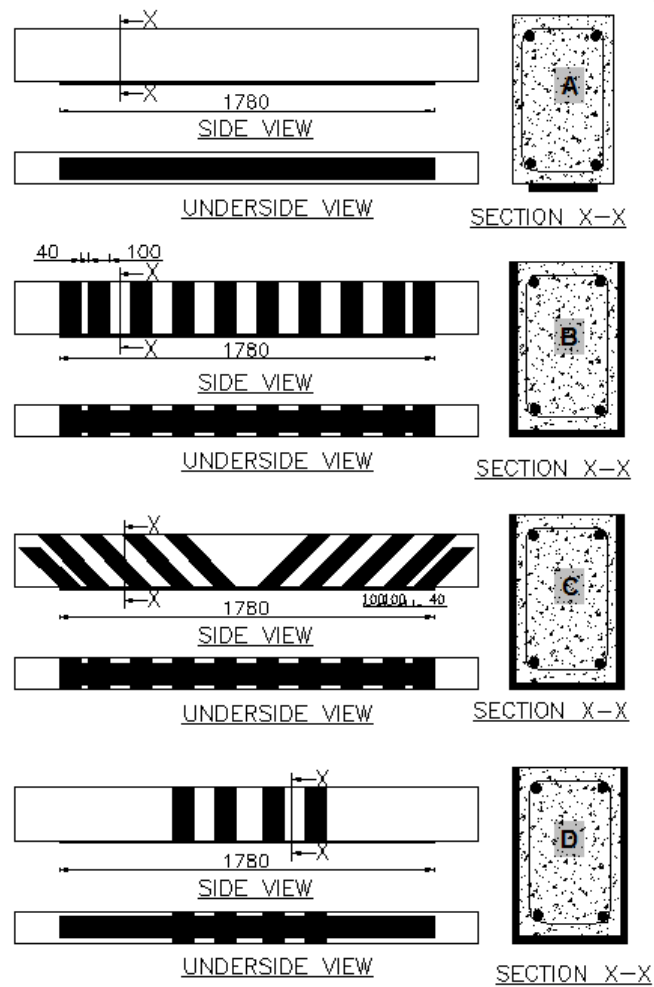


Figure 2 Wrapping scheme A/B/C/D

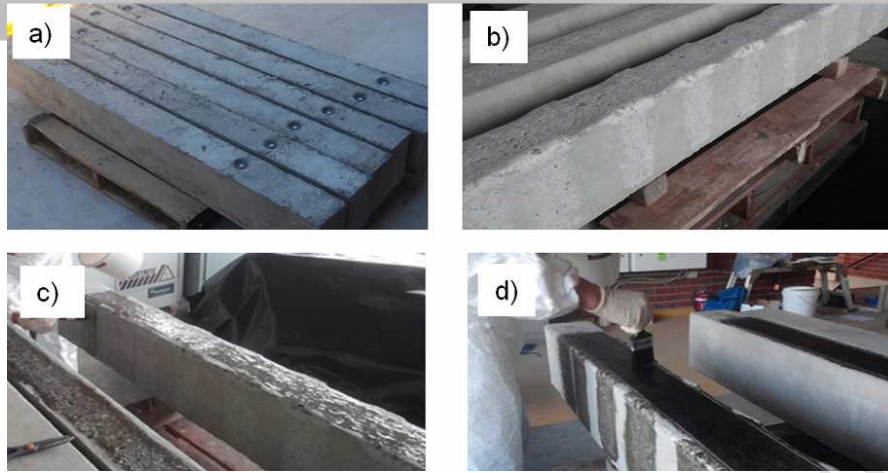


Figure 3 (a) Casted beams; (b) Edges rounded and surface roughened; (c) Priming of the roughened concrete surface (d) Wet layup of BFRP strips

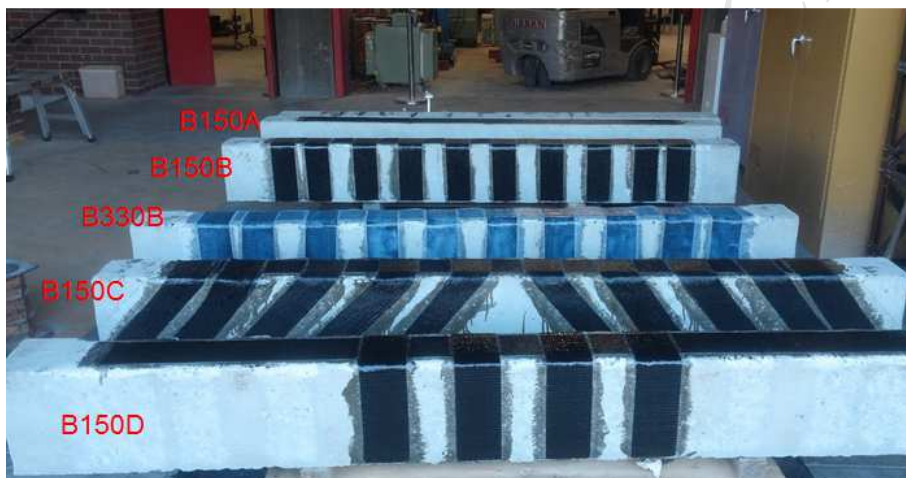


Figure 4 Testing specimens

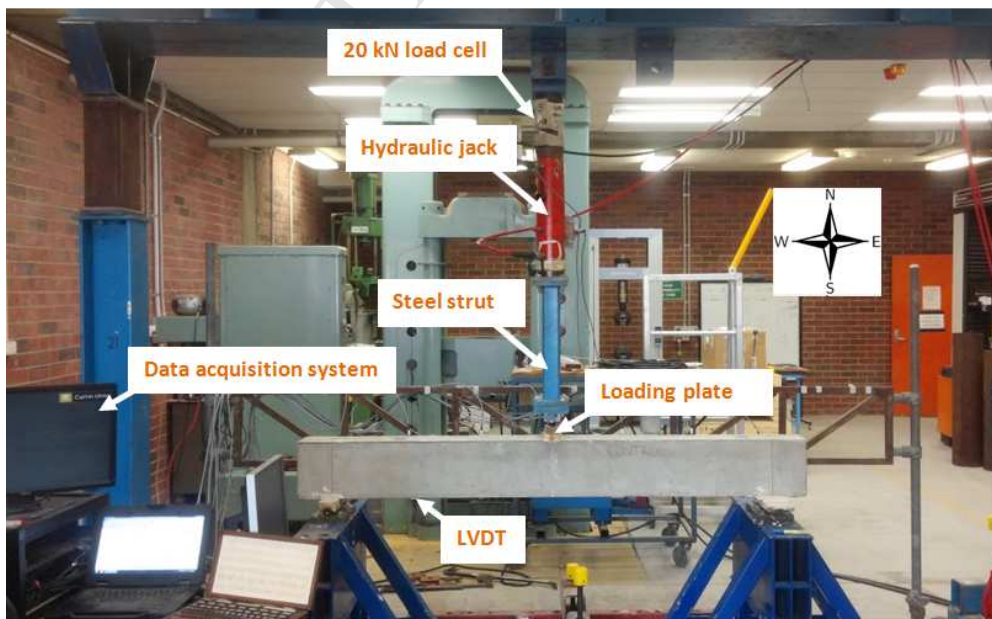


Figure 5 Three-point testing setup

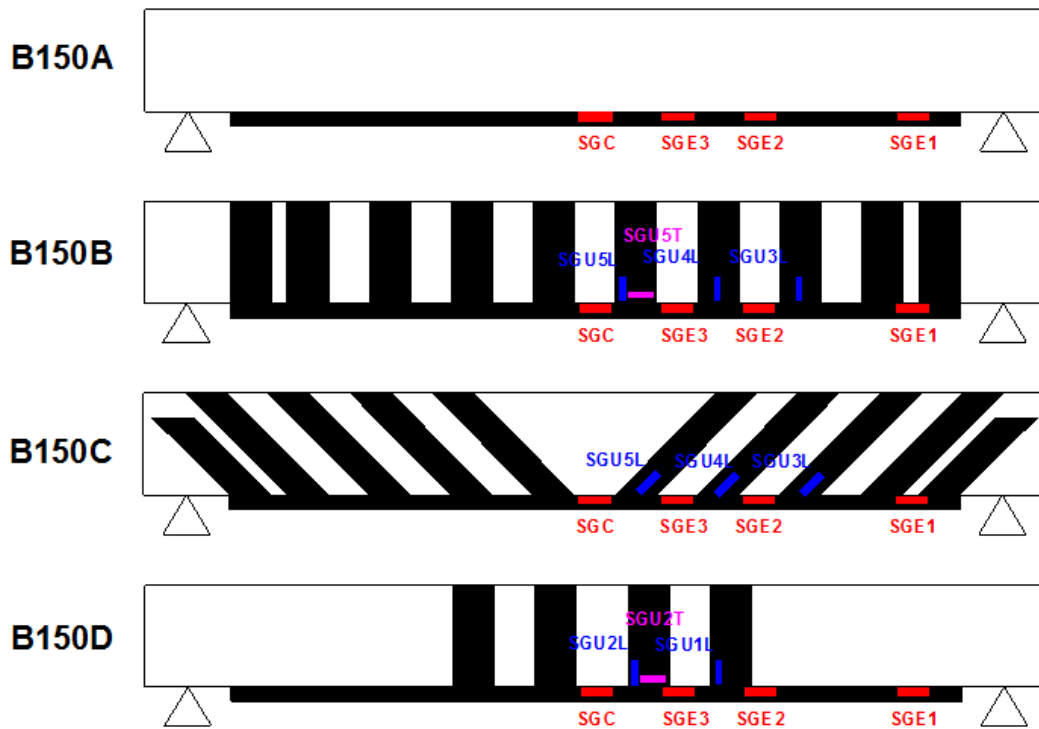


Figure 6 Installation of strain gauges

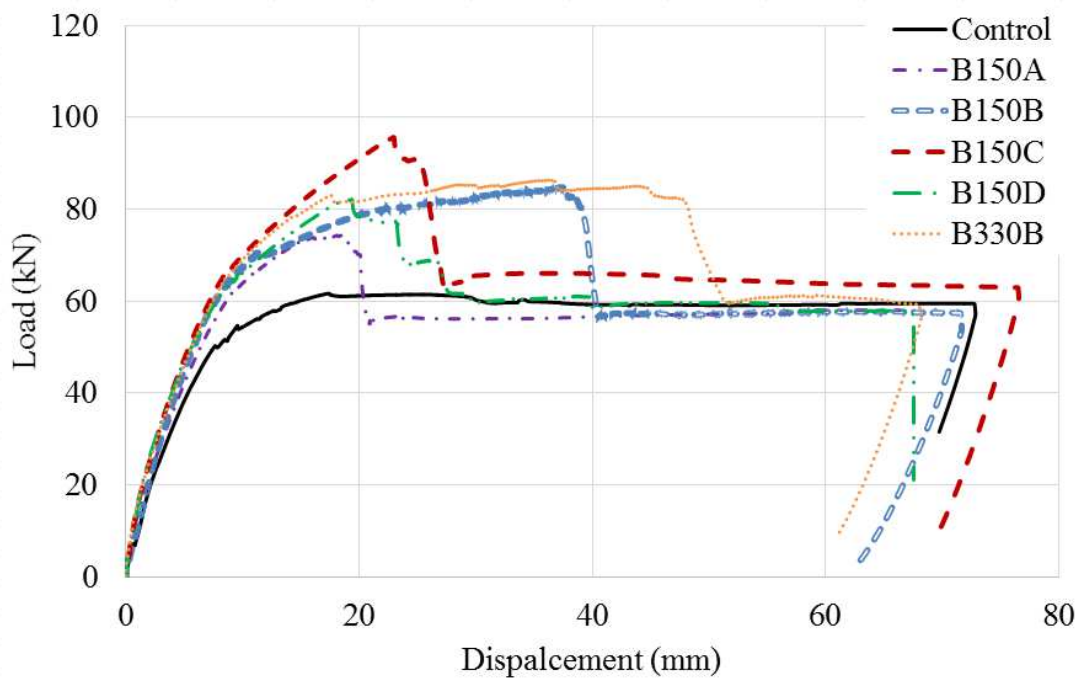


Figure 7 Load-displacement curves of all beams



Figure 8 (L) Early crack development of control specimen, (R) Crack development close to failure load of control specimen

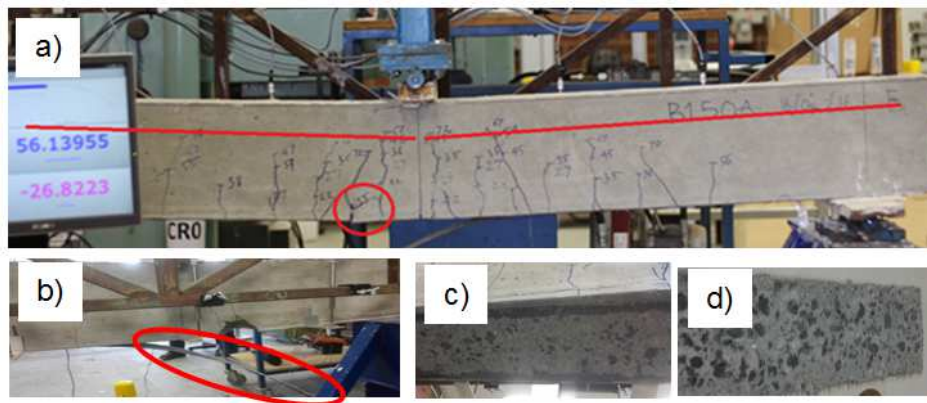


Figure 9 (a) Failure mode of specimen B150A (b) Debonded BFRP strip; (c) Concrete surface after debonding; (d) BFRP/concrete interface after debonding

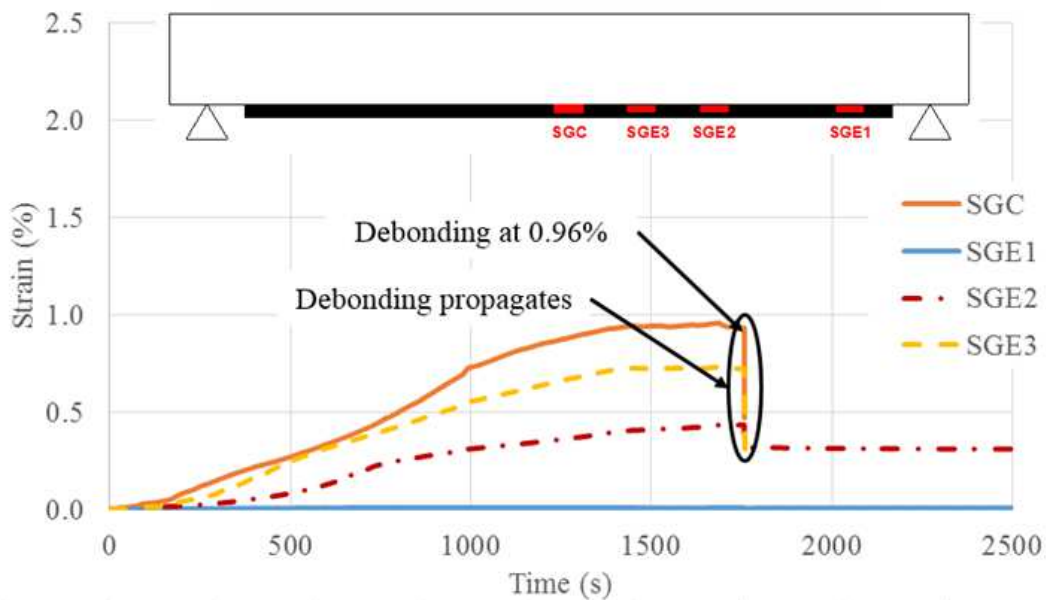


Figure 10 Strain-time histories of Beam B150A

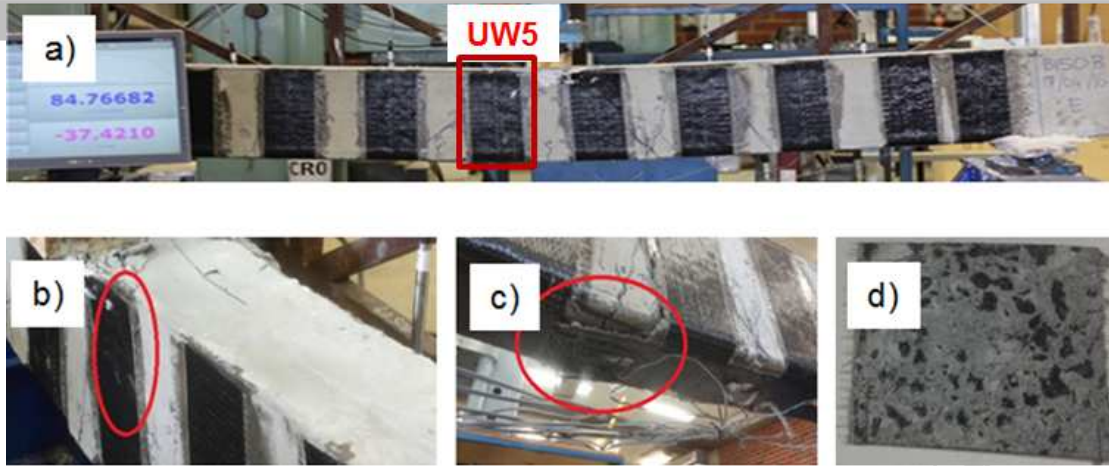


Figure 11 (a) Failure mode of Beam B150B; (b) U-jacket debonding; (c) Rupture of the soffit strip; (d) BFRP/Concrete interfacial failure of U-jacket UW5

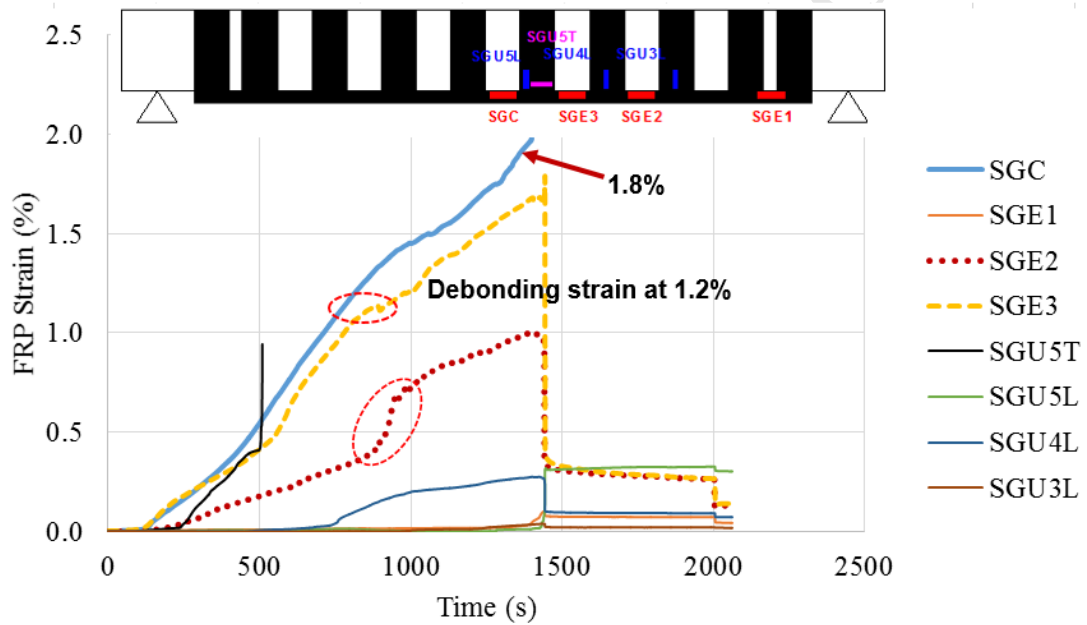


Figure 12 Strain-time histories of Beam B150B

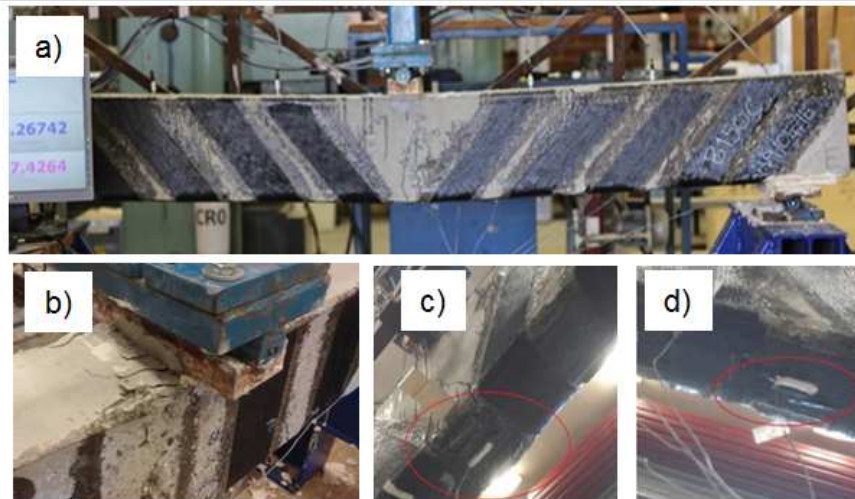


Figure 13 (a) Failure mode of Beam B150C; (b) Compressive failure of concrete at loading plate; (c) Complete BFRP rupture at mid-span; (d) Partial BFRP rupture at SGE3

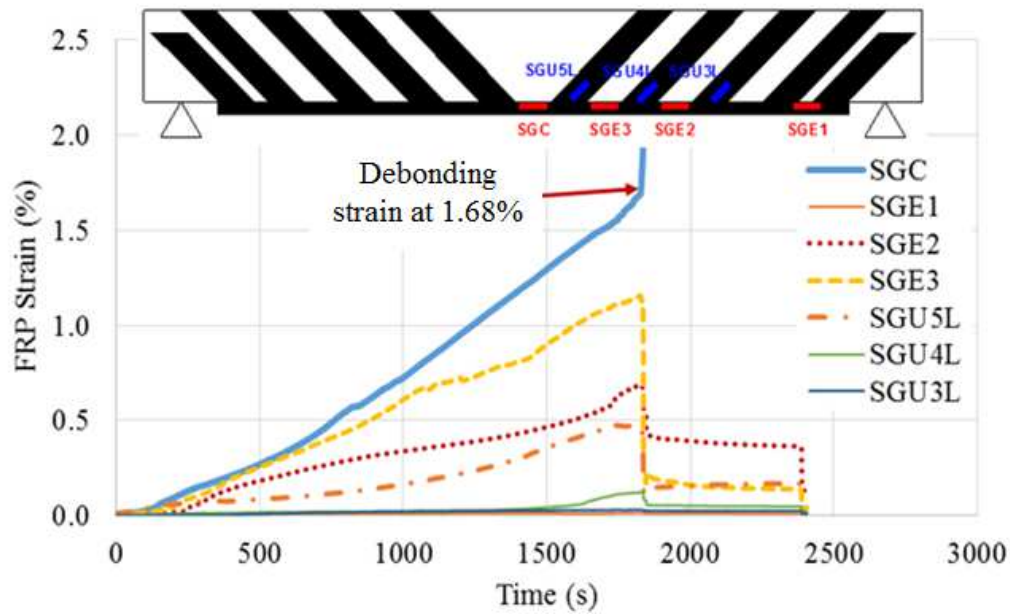


Figure 14 Strain-time histories of Beam B150C

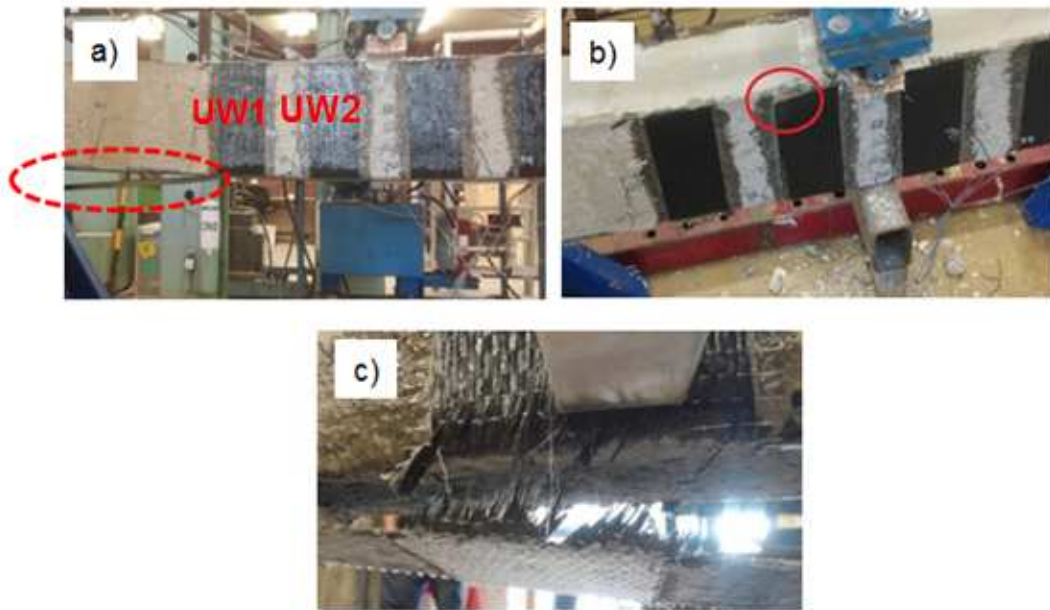


Figure 15 (a) Debonding of the BFRP soffit strip where no U-jacket anchorage; (b) Debonding of UW2 of B150D; (c) Rupture of UW1 at the edge of B150D



Figure 16 (a) Interfacial failure of the soffit strip, (b) Concrete cover separation of the U-jacket

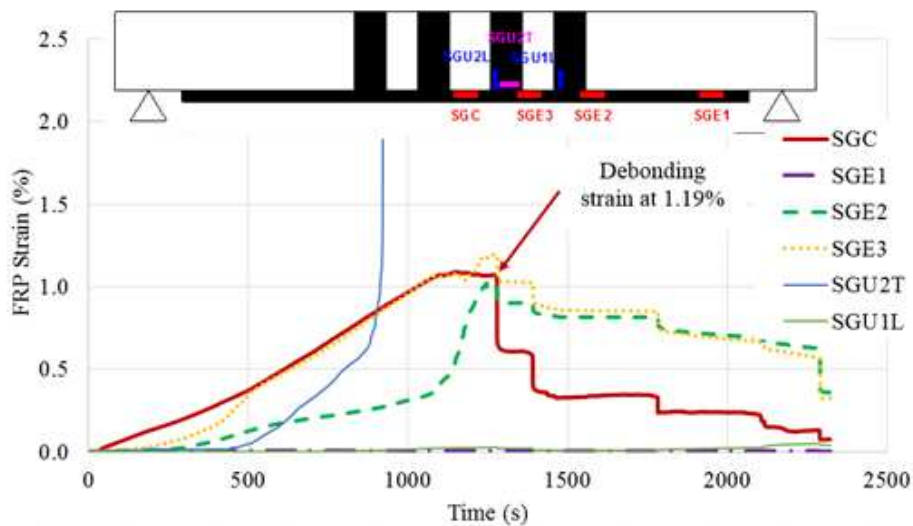


Figure 17 Strain-time histories of Beam B150D



Figure 18 (a) Intermediate crack induced interfacial debonding of soffit strip of B330B; (b) Complete failure of B330B by debonding of soffit strip and rupture of UE1, UE2 and UE3

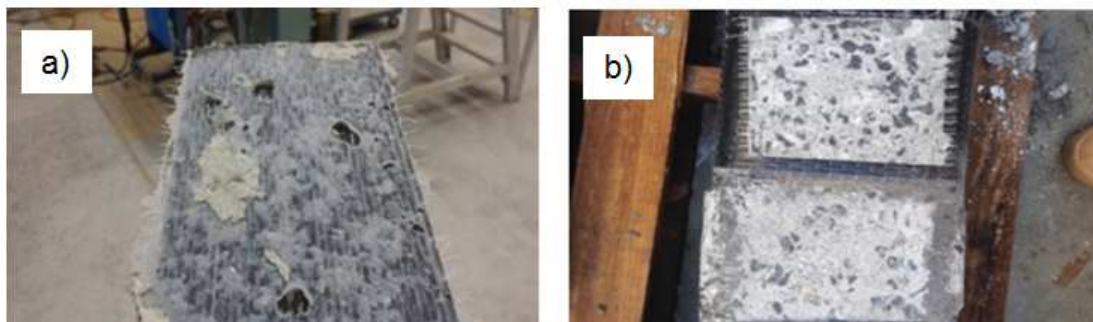


Figure 19 (a) Adhesive failure at BFRP/concrete interface of B330B, (b) Minimal damage to concrete substrate of B330B

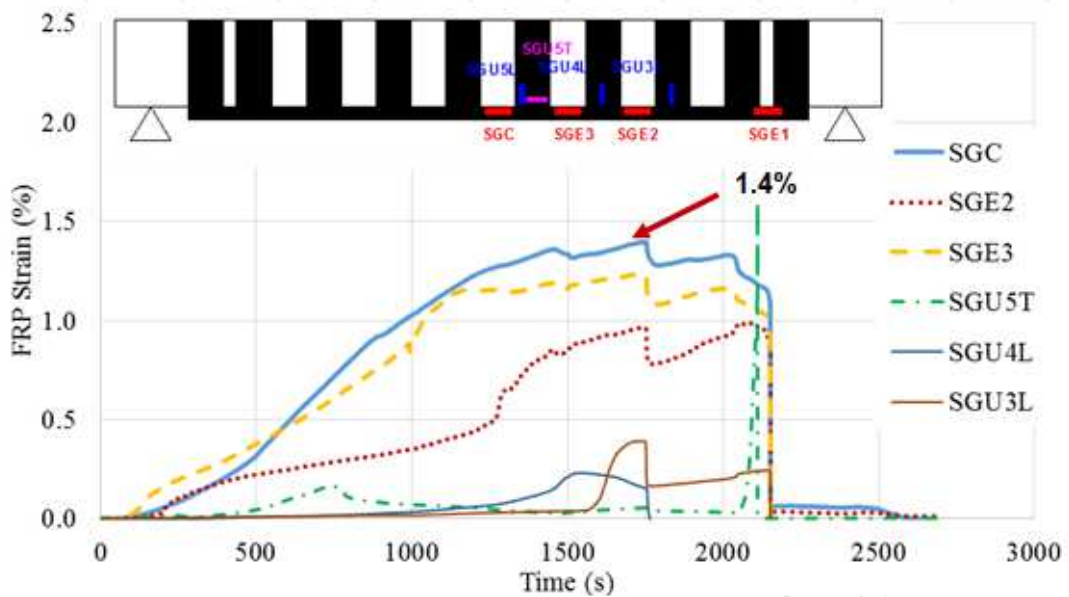


Figure 20 Strain-time histories of Beam B330B

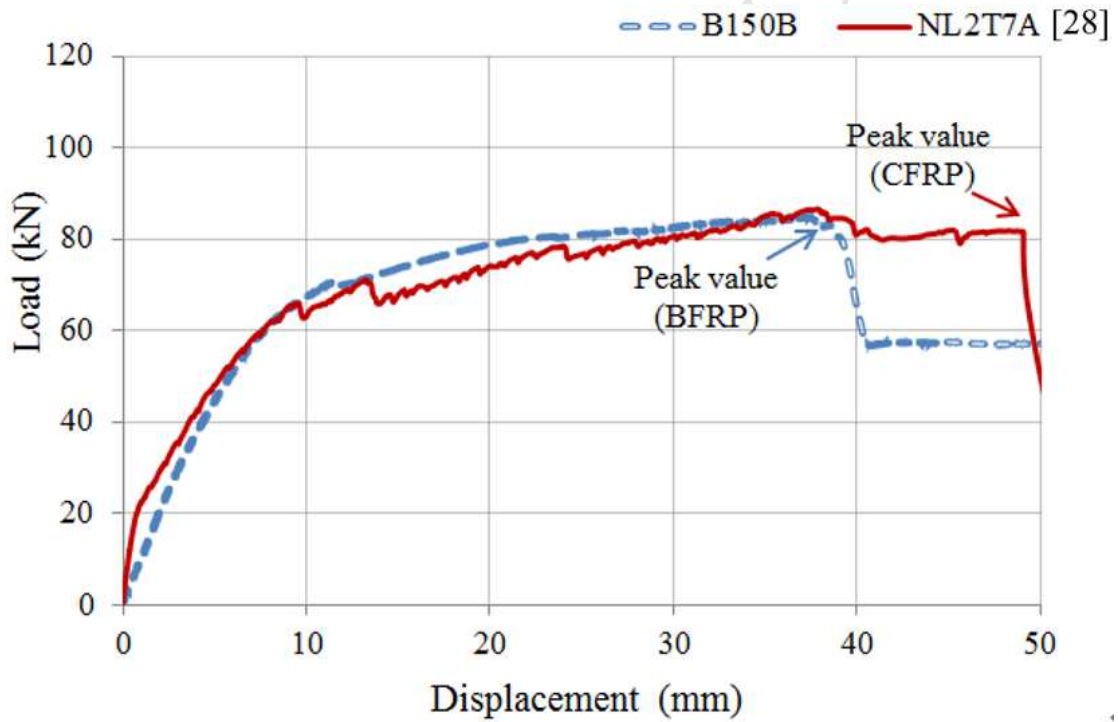


Figure 21 Load-displacement curves of BFRP strengthened beam B150B and CFRP strengthened beam NL2T7A [28]

- Very limited study on RC beams strengthened by BFRP is available.
- The effect of various BFRP wrapping schemes on the flexural performance is studied.
- The effect of U-jacket anchorage on BFRP strengthening performance is analyzed.
- The effect of epoxy adhesives on the flexural capacity of RC beams is investigated.
- The predication on BFRP strengthening by using ACI 440.2R-08 is verified.